ADAPTIVE ALGORITHMS AND EXPERIMENTAL RESULTS OF A BOLUS CHASING CT SCANNER

H. Bai [*],[***] **S. Remersaro** [**] **J. Bennett** [*]
J. Halloran [****] **J. Meinel** [*] **J. Bodmer** [**]
M. Sharafuddin [*] **M. Vannier** [†] **G. Wang** [*]
E.W. Bai [**],[‡]

[*] *Dept of Radiology, University of Iowa*
[**] *Dept. of Elec and Comp Engineering, University of*
Iowa, Iowa City, Iowa, 52242, USA
[***] *West High School, Iowa City, Iowa*
[****] *Dept of Interventional Radiology, Cedar Vally Medical*
Specialists, Waterloo, Iowa
[†] *Dept of Radiology, University of Chicago, Chicago*
[‡] *Corresponding author, er-wei-bai@uiowa.edu*

Abstract: In this paper, an adaptive scheme is proposed for a next generation CT scanner. The purpose of the control is to estimate the contract bolus position so its variations can be compensated by moving the patient table. The convergence result has been achieved and the experimental results are very promising. *Copyright$^{©}$ 2005 IFAC*

Keywords: adaptive control, identification, nonlinear systems

1. INTRODUCTION

In the recent years, CT (Computed Tomography) angiography has become one of the most popular medical diagnostic tools (Rubin *et al.*, 1998) due to its non-invasive nature and faster scanning capabilities. In CT angiography, contrast material is often administrated to allow a narrow temporal window to obtain optimal visualization of vessels, lesions and tumors (Kormano *et al.*, 1983; Sheafor *et al.*, 1998; Tublin *et al.*, 1999). The quality of scans depends on the ability to synchronize patient table position with the relatively narrow aperture of the imaging system during propagation of a contrast bolus after intravenous injection. Contrast bolus synchronization is achieved by using arrival monitoring with CT fluoroscopy. However, arrival monitoring synchronizes only the initial peak of contrast and the subsequently as-

sumed linear table velocity becomes problematic as time increases.

There is abundant literature on fluid mechanics and its applications including physiology (Bassingthwaighte *et al.*, 1992; Kroll *et al.*, 1996), pharmacokinetics (Nadler and Hidalgo, 1965), and biomedical engineering (Chandran, 1992; Goldsmith and Lewis, 1996). Several clinical studies of CT contrast enhancement have been published (Sheafor *et al.*, 1998; Berland, 1995; Kopka *et al.*, 1996). Bolus dynamics are complex and influenced by contrast administration protocol and patient characteristics (age, sex, weight, height, cardiovascular status, renal function, etc.) (Sheafor *et al.*, 1998). Peak bolus velocity is rarely uniform. Therefore synchronization of the bolus with a fixed, preset table transport often results in less-desirable vascular enhancement. Lack of

synchronization may be more problematic when scanning speed is fast, contrast volume is small, injection rate is high (leading to reduced peak duration), and/or variable vessel lumen diameter. Even for a normal individual, it is common that the contrast bolus velocity is rapid in the torso and relatively slow in the legs. Moreover, if asymmetric peripheral vascular disease exists, there may also be substantial variability in flow velocity between the opposite legs. Scanning too early may result in over-estimation of stenosis, while scanning too late may result in venous opacification. The published data shows that even in a normal person, the bolus velocities at different body section can vary by 8 times, see Table 1. Obviously, adaptive bolus chasing techniques are relevant to CT angiography because of the impact on image quality, as well as the need to limit contrast dose and radiation exposure.

To overcome these problems, three methods were developed in the literature to individualize scan timing during constant-speed spiral CT angiography (Schweiger *et al.*, 1998): (1) test bolus timing, (2) ROI threshold triggering, and (3) visual cue triggering. The test bolus method may decrease lesion conspicuity due to equilibration by the test bolus (Kopka *et al.*, 1996; Hubener *et al.*, 1982). The two triggering methods are vulnerable to patient motion, usually related to breathing, which may displace the target organ or vessel from the scan plane (Kopka *et al.*, 1996; Schweiger *et al.*, 1998; Silverman *et al.*, 1996). The fundamental limitation of all three methods is the inability to match the table translation to the bolus propagation. Another factor not considered is that fluid velocities surge during systole and are relatively stationary during diastole.

Our aim is to develop an adaptive bolus chasing CT angiography technique. The idea is illustrated in Figure 1. The control system consists of an imaging acquiring, processing and reconstruction part, an adaptive algorithm to estimate and predict future bolus position and a controller that moves the patient table to compensate the bolus variations. Works reported here are the algorithm development and experimental results in a clinical environment based on the published clinical data in Table 1. The convergence of the algorithm has been achieved and the experimental results show very promising results of the adaptive techniques applied to CT angiography.

2. CONTROLS AND ESTIMATION ALGORITHMS

The control goal is to move the patient table by the the exact amount as the bolus but in opposite direction so that the bolus and the imaging aperture are synchronized.

Let $p_i = p(i\Delta t)$ be the bolus position at time t and $v_i = v(i\Delta t)$ be the average velocity of the bolus between two consecutive sampling instances t and $t + \Delta t$, where Δt is the sampling period. Clearly,

$$p_{i+1} = p_i + v_i \Delta t$$

Should the bolus position p_{i+1} at time $(i + 1)\Delta t$ be available in advance at time $i\Delta t$, the controller would move the patient table to p_{i+1} at time $(i + 1)\Delta t$. The difficulty is that p_{i+1} is unknown at time $i\Delta t$ and has to be estimated based on p_k's and v_k's, $k \leq i$, or their estimates. As illustrated conceptually in Figure 1, the overall control system consists of 4 components. The first part is imaging acquiring and processing that provides real time bolus position. The second part is a predictor. Based on some bolus dynamics models and observed measurements, it predicts future bolus positions. Since the bolus dynamics is unknown, the model inevitably involves some unknown parameters. Thus, the estimator is the third part that estimates unknown parameters online. The final part is a patient table driven by a motor. The motor takes information from the predictor and moves the table so that the imaging aperture and the bolus are synchronized.

Clearly, an accurate estimation and prediction of the future bolus position based on the current and past bolus information is essential. The success of the proposed strategy depends on how accurately the model can predict. Therefore, modeling is an important step in estimating and predicting the bolus position.

Full models

It was shown (Wang *et al.*, 2000*c*) that bolus propagation is governed by a set of very large number of partial differential equations which contains a large number of patient and circulatory stage-dependent parameters. The model is fairly accurate provided that all parameters are available. Because these parameters are unknown, this full model has a little use in practice for adaptive bolus chasing CT angiography. It is known in the adaptive community that partial differential equations are not easy to deal with. Morover, online estimation of such a large number of parameters in a very short time (typically CT angiography lasts about 20-30 seconds) is impossible. Another commonly used model to describe bolus dynamics is the compartmental model (Bae *et al.*, 1998) that is also of little use for adaptive bolus chasing CT angiography. Again, the model is a set of equations involving a large number of unknown parameters that are patient and circulatory stage dependent. Obviously, parameters about the patient vessel radius at each stage of the vascular tree

Blood Velocities	Peak Velocity (cm/s)	Mean Velocity (cm/s)	Diameter (cm)
Aorta	150 ± 30	27 ± 8.9	1.8 ± 0.2
Common Iliac artery	$125 \pm NA$	13.5 ± 4.0	$0.9 \pm NA$
External Iliac artery	119 ± 21.7	10.5 ± 5.0	0.79 ± 0.13
Common Femoral artery	114 ± 24.9	10.2 ± 4.8	0.82 ± 0.14
Superficial Femoral artery	90.8 ± 13.6	8.8 ± 3.5	0.60 ± 0.12
Popliteal artery	68.8 ± 3.5	4.9 ± 2.9	0.52 ± 0.11
Posterior tibial artery	61 ± 20	4.4 ± 3.3	$0.25 \pm NA$
Dorsalis pedis artery	NA	3.6 ± 3.8	$0.2 \pm NA$

Table 1. Blood velocity variation for a normal male adult

are difficult to have in advance. Also, disease-state related parameters are impossible to be quantified prior to an angiogram. Also, the compartmental model describes contrast enhancement specific to a compartment (organ or vessel) (Bae *et al.*, 1998) instead of predicting the bolus dynamic as a function of time.

Extended Hammerstein models

To overcome this difficulty, we proposed a simplified nonlinear model, called the extended Hammerstein model in our previous works (Bennett *et al.*, 2003). The idea is that within each body section, the bolus propagation can be modeled by a linear system, provided that the pulsatility of the blood flow is not very strong. For instance at a fixed location y, from (Bassingthwaighte *et al.*, 1966), the bolus dynamics can be described by convolutions of three functions

$$b(t,y) = c(t) * \frac{1}{\sigma(y)\sqrt{2\pi}} e^{-\frac{(t-t_c(y))^2}{2\sigma^2(y)}} * \frac{1}{\tau(y)} e^{\frac{t}{\tau(y)}}$$

where the function $c(t)$ is determined by the injection of the bolus and the parameters t_c, τ and σ depend on the location y, i.e., the body section.

Clearly, the overall system is a nonlinear system that consists of several linear systems which switch from one to another depending on the body section. If the body is divided into three sections, the extended Hammerstein model consists of three linear systems

$$b(t,y_1), b(t,y_2), b(t,y_3)$$

for $y \neq y_1, y_2, y_3$, $b(t,y)$ can be obtained by interpolation. The difference between this model and the traditional Hammerstein model is that the nonlinearity acts like a switching function depending on external conditions. If the parameters σ, τ and t_c can be estimated, the complete dynamics of the bolus is available and in turn, the next bolus position is obtained. A difficulty of this model is that the pulsatility is usually strong. The blood surges in the systole phase and is smooth in the diastole phase. Thus, to capture the pulsatility, the systole and diastole phases have to be separated. This adds complexity to the model and requires additional physiological measurements. For instance, to determine whether it is in the systole or diastole phase, additional EKG signal has to

be provided which may or may not be the case in reality.

Non-parametric models

What we are interested is not complete dynamics of the bolus but to be able to predict the next bolus position. Though the bolus velocity varies greatly, with current computer and CT techniques, the difference of the bolus positions at two consecutive sampling instances is extremely small provided that the sampling rate is high. In fact, the bolus velocity may be considered as a constant between two sampling instances if the sampling interval is small. With the knowledge of the current bolus velocity which is the difference between the current and the immediate past bolus positions divided by the sampling interval, the next (future) bolus peak position can be fairly accurately predicted. To estimate the velocity, only one parameter, the bolus position at the current time that is patient and circulatory stage-dependent, needs to be estimate. Moreover, this information can be readily obtained in modern CT systems (Wang *et al.*, 2000a; Wang *et al.*, 2000b). Therefore, based on this very simple adaptive nonlinear model, the future bolus position can be estimated and predicted. Results reported in this paper is based on this non-parametric model.

We now use the idea of the above non-parametric model to define an adaptive algorithm to estimate p_{i+1}. Though the bolus velocity v_i depends on i and is unknown, with a very short sampling period Δt, two consecutive v_i and v_{i-1} are very close and differ by only a very small amount. We assume in this paper that there exists a small $\delta > 0$ so that

$$v_{i-1} - v_i = \Delta_i, \quad |\Delta_i| \leq \delta \quad \forall i$$

Now, let $\hat{v}_i$ and $\hat{p}_i$ denote the estimates of v_i and p_i at time $i\Delta t$, respectively, and define the the adaptive estimation algorithm

$$
\begin{aligned}
\hat{v}_i &= \hat{v}_{i-1} + \mu(p_i - p_{i-1} + e_i - \hat{v}_{i-1}\Delta t) \\
\hat{p}_{i+1} &= p_i + \hat{v}_i \Delta t
\end{aligned}
\tag{1}
$$

where $\mu > 0$ is the gain. Since p_i and p_{i-1} are measurements from a camera, noises are unavoidable denoted by e_i. The hope is that $\hat{p}_i$ converges to p_i asymptotically if $e_i, \delta = 0$ and is close to p_i if e_i and δ are not zero but small.
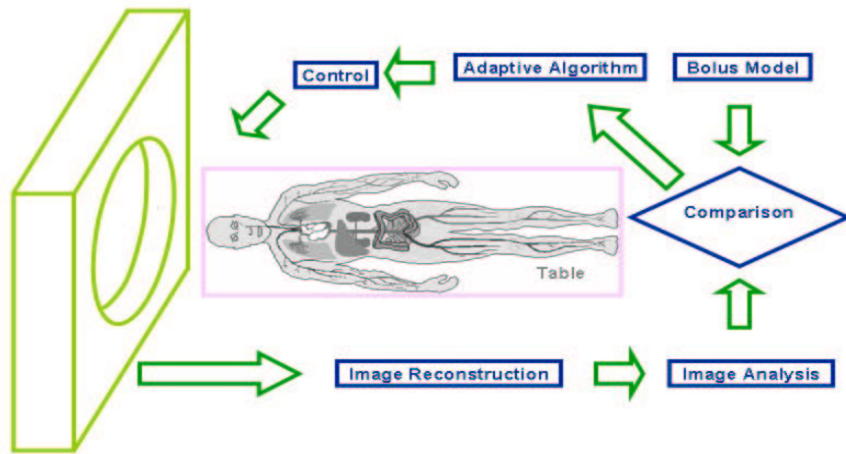
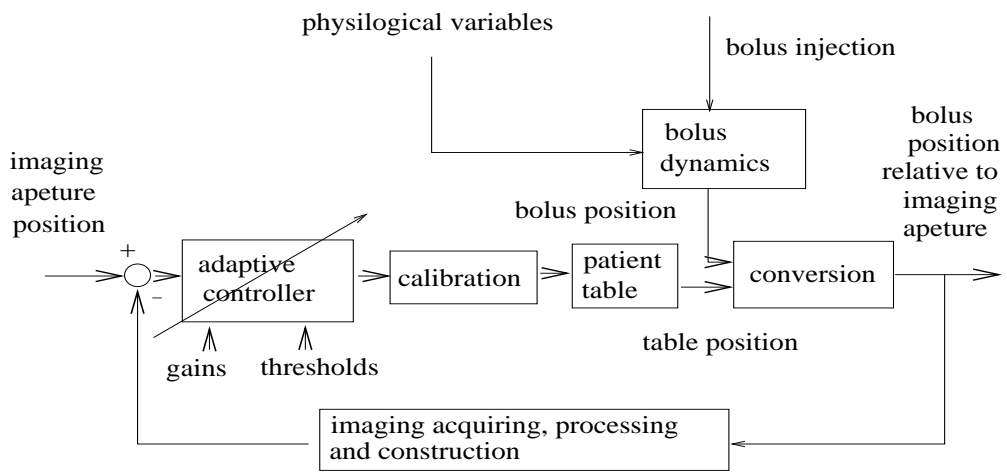Fig. 1. Control scheme illustration

Fig. 2. Block diagram of the adaptive control
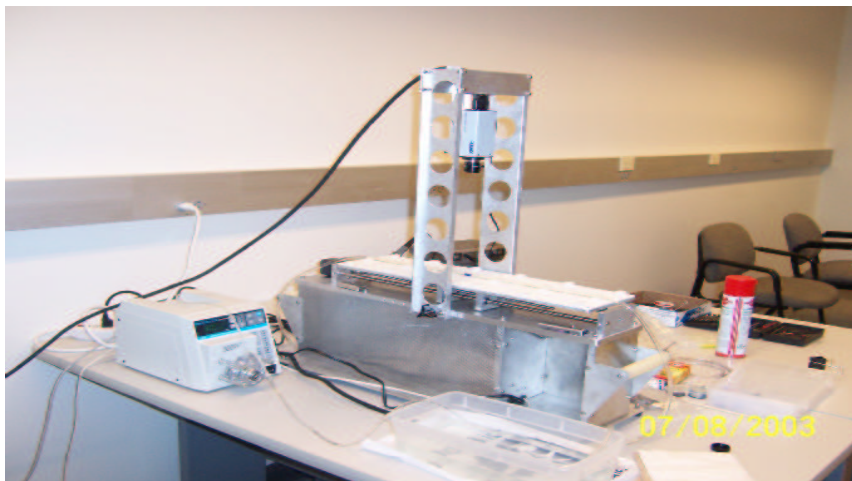

Fig. 3. Experimental setup

3. CONVERGENCE ANALYSIS

Let the estimation errors at time $i\Delta t$ be,

$$\tilde{v}_i = \hat{v}_i - v_i$$
$$\tilde{p}_i = \hat{p}_i - p_i = (p_{i-1} + \hat{v}_{i-1}\Delta t)$$
$$= -(p_{i-1} - v_{i-1}\Delta t)\tilde{v}_{i-1}\Delta t$$

Then, the error equations are given by

$$\begin{aligned}\tilde{v}_i &= (1-\mu\Delta t)\tilde{v}_{i-1} + \Delta_i + \mu e_i\\ \tilde{p}_{i+1} &= (1-\mu\Delta t)\tilde{p}_i + \Delta_i\Delta t + \mu\Delta t e_i\end{aligned}$$

Theorem 3.1. Consider the adaptive algorithm (1). Suppose $|1-\mu\Delta t| < 1$. Then,

(1) In the absence of noise, the estimation error $\tilde{p}_k$ asymptotically satisfies

$$|\tilde{p}_k| \leq \frac{\delta}{\mu}$$

(2) If the noise is iid with zero mean and variance σ_e^2, then

$$|\mathbf{E}\tilde{p}_k| \leq |(1-\mu\Delta t)^k \tilde{p}_0| + |\sum_{i=0}^{k-1}(1-\mu\Delta t)^{k-1-i}$$

$$\cdot\delta\Delta t| + |\sum_{i=0}^{k-1}(1-\mu\Delta t)^{k-1-i}\mu\Delta t \mathbf{E}e_i|$$

$$\Longrightarrow |\sum_{i=0}^{k-1}(1-\mu\Delta t)^{k-1-i}\delta\Delta t| \leq \frac{\delta}{\mu}$$

and

$$\mathbf{E}\tilde{p}_i^2 \Longrightarrow \{\sum_{i=0}^{k-1}(1-\mu\Delta t)^{k-1-i}\Delta_i\Delta t\}^2$$

$$+\sum_{i=0}^{k-1}[(1-\mu\Delta t)^2]^{k-1-i}\mu^2\Delta t^2\sigma_e^2$$

$$\leq (\frac{\delta}{\mu})^2 + \frac{\mu\Delta t\sigma_e^2}{2-\mu\Delta t}$$

where $\mathbf{E}$ stands for the expectation operator.

Proof: The results follows easily from the facts that

$$\tilde{p}_k = (1-\mu\Delta t)^k\tilde{p}_0 + \sum_{i=0}^{k-1}(1-\mu\Delta t)^{k-1-i}\Delta_i\Delta t$$

$$+\sum_{i=0}^{k-1}(1-\mu\Delta t)^{k-1-i}\mu\Delta t e_i$$

and the first term decays exponentially, provided $0 < \mu\Delta t < 1$. This finishes the proof.

Remarks:

(1) The estimate $\hat{p}_k$ is biased but the bias is very small ($\leq \frac{\delta}{\mu}$). This bias is unavoidable if the variations Δ_i's of v_k's unknown.
(2) To make the bias $\frac{\delta}{\mu}$ small $\Longrightarrow \mu$ large.
(3) To increase the convergence rate $\Longrightarrow 1-\mu\Delta t$ small $\Longrightarrow \mu\Delta t$ close to 1.
(4) To make $\frac{\mu\Delta t\sigma_e^2}{2-\mu\Delta t}$ small $\Longrightarrow \mu\Delta t$ small.

Thus, there is a compromise in choosing the gain μ. Once the estimate $\hat{v}_i$ is available, the next bolus position can be estimated

$$\hat{p}_{i+1} = p_i + \hat{v}_i\Delta t$$

and the controller moves the table to $\hat{p}_{i+1}$ at time $(i+1)\Delta t$. The block diagram of overall control system is shown in Figure 2.

4. EXPERIMENTAL RESULTS

The proposed adaptive control algorithm has been implemented on a prototype CT scanner shown in Figure 3. This prototype consists of four elements: a Master Flex Pump 7550-30, a movable table controlled by a Vexta α stepping motor AS46, a Pulnix-6700 camera and a PC (personal computer). The pump is controlled by the PC that simulates a person's heart which drives the bolus through plastic tubings. The bolus velocity can be arbitrarily assigned by computer programs. The stepping motor takes commands from the PC through a serial port. This simulates the patient table. The camera, connected to the PC by a PCI card, provides the real time bolus position that simulates the CT imaging device. The imaging acquiring and processing are carried by NI IMAQ VISION DEVELOPMENT MODULES. In fact, all the algorithms are implemented by using the NI Labview software which is widely available. The experimental results are shown in Figures 4 and 5. In Figure 4, the actual bolus position (solid line) and the controlled table position (dotted line) are shown. There are almost indistinguishable. Figure 5 shows the tracking error (mm) which is the difference between the actual bolus position and the controlled table position or equivalently, the difference between the imaging aperture and the actual bolus position. Clearly, the proposed adaptive control algorithm in this paper performs very well and the maximum tracking error is within 4mm.

5. CONCLUDING REMARKS

In this paper, preliminary experimental results have been obtained for adaptive control of a next generation of CT scanner. The control scheme combines the imaging techniques, adaptive estimation algorithms and controls. The experimental data shows that the bolus position can be accurately estimated and predicted by using a simple non-parametric model which does not requires much computations and needs to estimate only one parameter, either the velocity or the position of the bolus.

REFERENCES

Bae, K, J Heiken and J Brink (1998). Aortic and hepatic contrast medium enhancement at ct:

Part iii. effect of contrast medium injection rate - pharmacokinetic analysis and experimental porcine model. *Radiology* **207**, 647–655.

Bassingthwaighte, A, FH Ackerman and EH Wood (1966). Application of the lagged normal density curve as a model for arterial dilution curves. *Circulation Research* **XVIII**, 398–415.

Bassingthwaighte, J, I Chan and C Wang (1992). Computationally efficient algorithms for capillary convection-permeation-diffusion models for blood-tissue exchange. *Ann. Biomed. Eng* **20**, 687–725.

Bennett, J, EW Bai, J Halloran and G Wang (2003). A preliminary study on adaptive field-of-view tracking in peripheral digital subtraction angiography. *J. of X-ray Science and Technology* **11**, 149–159.

Berland, L (1995). Slip-ring and conventional dynamic hepatic ct: Contrast material and timing considerations. *Radiology* **195**, 1–8.

Chandran, KB (1992). Cardiovascular biomechanics. *New York City, NY: New York University Press.*

Goldsmith, W and E Lewis (1996). Introduction to bioengineerin. *Oxford, UK: Oxford University Press.*

Hubener, K, W Kalender and H Metzger (1982). Fast digital recording of x-ray dilution curves: A preliminary evaluation. *Radiology* **145**, 545–547.

Kopka, L, J Rodenwaldt, U Fischer, D Mueller and J Oestmann E Grabbe (1996). Dual-phase helical ct of the liver: Effects of bolus tracking and different volumes of contrast material. *Radiology* **201**, 321–326.

Kormano, M, K Partenen, S Soimakallio and T Kivimaki (1983). Dynamic contrast enhancement of the upper abdomen: Effect of contrast medium and body weight. *Investigative Radiology* **18**, 364–367.

Kroll, K, N Wilke, M Jerosch-Herold, Y Wang, Y Zhang and et al (1996). Modeling regional myocardial flows from residue function of an intravascular indicator. *Am. J. Physio* **271**, H1643–1655.

Nadler, S and J Hidalgo (1965). Blood volume. *In: Sevelius G, editor. Radioisotopes and circulation.*

Rubin, G, D Paik, P Johnston and S Napel (1998). Measurement of the aorta and its branches with helical ct. *Radiology* **206**, 823–829.

Schweiger, G, P Chang and B Brown (1998). Optimizing contrast enhancement during helical ct of the liver: A comparison of two bolus tracking techniques. *AJR* **171**, 1551–1558.

Sheafor, D, M Keogan, D DeLong and R Nelson (1998). Dynamic helical ct of the abdomen: Prospective comparison of pre- and postprandial contrast enhancement. *Radiology* **206**, 359–363.

Silverman, P, S Roberts, I Ducic, M Tefft, M Olson, C Cooper and et al (1996). Assessment of a technology that permits individualized scan delays on helical hepatic ct: A technique to improve efficiency in use of contrast material. *AJR* **167**, 79–84.

Tublin, M, F Tessler, S Cheng, T Peters and P McGovern (1999). Effect of injection rate of contrast medium on pancreatic and hepatic helical ct. *Radiology* **210**, 97–101.

Wang, G, C Crawford and W Kalender (2000a). Multirow detector and cone-beam spiral/helical ct. *IEEE Trans. Med. Imaging* **19**, 817–821.

Wang, G, G Raymond and et al (2000b). A model of intravenous bolus propagation for optimization of contrast enhancement. *SPIE.*

Wang, G, G Raymond, Y Li, D Schweiger, K Sharafuddin, A Stolpen, S Yang, Z Li, J Bassingthwaighte, B James and M Vannier (2000c). A model on intervenous bolus propagation for optimization of contrast enhancemen. *Proceedings of SPIE - The International Society for Optical Engineering* **3978**, 436–437.
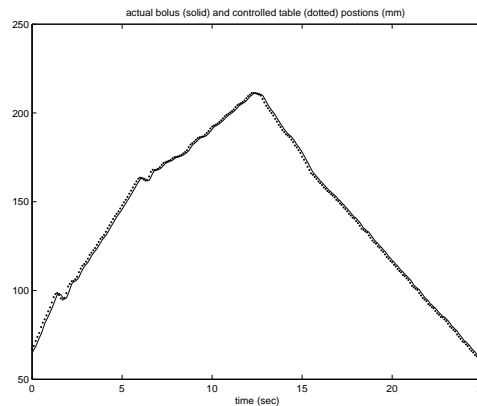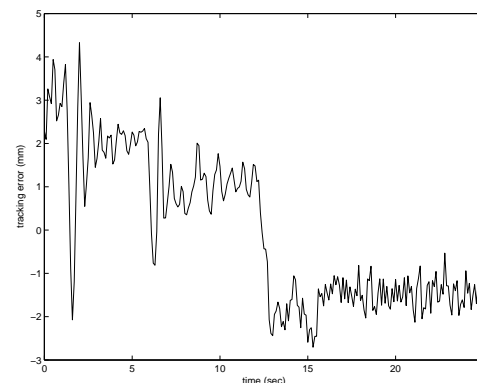
Fig. 4. The actual bolus position(solid) and the controlled table position (dotted)

Fig. 5. Tracking error(mm)